


Protein Disulfide Isomerase Inhibition Synergistically Enhances the Efficacy of Sorafenib for Hepatocellular Carcinoma

Jae-Kyung Won,^{1-3*} Su Jong Yu,^{4*} Chae Young Hwang,^{1*} Sung-Hwan Cho,¹ Sang-Min Park,¹ Kwangsoo Kim,⁵ Won-Mook Choi,⁴ Hyeki Cho,⁴ Eun Ju Cho,⁴ Jeong-Hoon Lee ,⁴ Kyung Bun Lee,³ Yoon Jun Kim,⁴ Kyung-Suk Suh,⁶ Ja-June Jang,³ Chung Yong Kim,⁴ Jung-Hwan Yoon,^{4**} and Kwang-Hyun Cho^{1,2**}

Sorafenib is the only approved targeted drug for hepatocellular carcinoma (HCC), but its effect on patients' survival gain is limited and varies over a wide range depending on pathogenetic conditions. Thus, enhancing the efficacy of sorafenib and finding a reliable predictive biomarker are crucial to achieve efficient control of HCCs. In this study, we utilized a systems approach by combining transcriptome analysis of the mRNA changes in HCC cell lines in response to sorafenib with network analysis to investigate the action and resistance mechanism of sorafenib. Gene list functional enrichment analysis and gene set enrichment analysis revealed that proteotoxic stress and apoptosis modules are activated in the presence of sorafenib. Further analysis of the endoplasmic reticulum stress network model, combined with *in vitro* experiments, showed that introducing an additional stress by treating the orally active protein disulfide isomerase (PDI) inhibitor (PACMA 31) can synergistically increase the efficacy of sorafenib *in vitro* and *in vivo*, which was confirmed using a mouse xenograft model. We also found that HCC patients with high PDI expression show resistance to sorafenib and poor clinical outcomes, compared to the low-PDI-expression group. **Conclusion:** These results suggest that PDI is a promising therapeutic target for enhancing the efficacy of sorafenib and can also be a biomarker for predicting sorafenib responsiveness. (HEPATOLOGY 2017;66:855-868).

Sorafenib, the first oral multikinase inhibitor, was approved for the treatment of hepatocellular carcinoma (HCC) a few years ago, but it has shown limited efficacy. Only a small fraction of patients (around 10%) show a clinical response to sorafenib, and, at most, 30%–40% of HCC patients demonstrate a disease control rate.⁽¹⁾ In the SHARP trial, the median

survival period was prolonged by sorafenib up to 3 months, but its benefit is not enough considering its high price and varying efficacy depending on patients.⁽²⁾

In general, a targeted anticancer drug should have a biomarker to predict its clinical response. Single kinase inhibitors, such as tarceva (epidermal growth factor receptor [EGFR] inhibitor) or crizotinib (anaplastic

Abbreviations: ALK, anaplastic lymphoma kinase; BCL2, B-cell lymphoma 2; BCLC, Barcelona Clinic Liver Cancer; cDNA, complementary DNA; CHOP, C/EBP homology protein; CI, confidence interval; CR, complete response; DCR, disease control rate; DMSO, dimethyl sulfoxide; EGFR, epidermal growth factor receptor; eIF2 α , eukaryotic initiation factor 2 α ; ER, endoplasmic reticulum; ERAD, ER-associated degradation; GADD34, growth arrest and DNA damage-inducible protein 34; GAPDH, glyceraldehyde 3-phosphate dehydrogenase; HCC, hepatocellular carcinoma; HR, hazard ratio; HSP, heat shock protein; IHC, immunohistochemistry; JNK, c-Jun N-terminal kinase; MANF, mesencephalic astrocyte-derived neurotrophic factor; mRECIST, modified Response Evaluation Criteria in Solid Tumors; ODE, ordinary differential equation; OS, overall survival; PD, progressive disease; PDI, protein disulfide isomerase; PERK, protein kinase RNA-like endoplasmic reticulum kinase; PI, propidium iodide; PR, partial response; ROC, receiver-operating characteristic; SD, stable disease; shRNA, short hairpin RNA; TTP, time to progression; UPR, unfolded protein response; VEGFR2, vascular endothelial growth factor receptor 2; XBP1, X-box binding protein.

Received November 3, 2016; accepted April 20, 2017.

Additional Supporting Information may be found at onlinelibrary.wiley.com/doi/10.1002/hep.29237/supinfo.

Supported by the National Research Foundation of Korea (NRF) grants funded by the Korea Government, the Ministry of Science, ICT & Future Planning (2015M3A9A7067220, 2014R1A2A1A10052404, 2013M3C8A1078501, and 2013M3A9A7046303), and a grant of the Korea Health Technology R&D Project through the Korea Health Industry Development Institute (KHIDI), funded by the Ministry of Health & Welfare, Republic of Korea (HI14C1277). The work was also supported by grants from the SNUH Research Fund (No. 03-2012-0390) and the Liver Research Foundation of Korea.

*These three authors equally contributed to this work.

**These two authors equally contributed to this work.

lymphoma kinase [ALK] inhibitor), have as predictive markers EGFR mutation and ALK translocation, respectively. However, such markers are still not available for sorafenib because it targets multiple kinases, including v-Raf murine sarcoma viral oncogene homolog B1, vascular endothelial growth factor receptor 2 (VEGFR2), platelet-derived growth factor receptor, FMS-like tyrosine kinase-3, rearranged during transfection, and cellular homolog of the feline sarcoma viral oncogene v-kit, complicating the mechanism of action.⁽³⁾ Thus, it is clinically important to investigate the mechanism of resistance to sorafenib and develop a new therapeutic strategy that can improve the efficacy of sorafenib.

To discover the action and resistance mechanism of sorafenib, we adopted systems approaches as follows: First, we analyzed mRNA expression changes in HCC cell lines in response to sorafenib and inferred that the endoplasmic reticulum (ER) stress pathway contributes to apoptosis driven by sorafenib. Second, based on these pathways, we constructed a network model and identified an apoptosis-promoting module as well as antiapoptotic modules upon sorafenib treatment. Then, using the network kernel analysis and *in silico* simulation based on the logic diagram and a computational model, we found that protein disulfide isomerase (PDI) can be a therapeutic target for enhancing the efficacy of sorafenib.

We further established that the combinatorial treatment of sorafenib and PDI inhibitor shows a synergistic effect *in vitro* and *in vivo*. In addition, we found that high PDI expression correlates with a poor response rate to sorafenib treatment and adverse clinical outcomes in the HCC patient cohort.

Taken together, these results suggest that PDI can be not only a useful predictive biomarker for sorafenib, but also a promising target for a combination therapy to overcome the resistance to sorafenib.

Materials and Methods

mRNA MICROARRAY EXPERIMENTS AND ANALYSIS

mRNA microarray experiments were performed in triplicate. HCC cell lines (SNU761, Huh7, Hep3B, and HepG2) were treated with sorafenib 3 μ M for 24 hours, whereas the control group was treated with only dimethyl sulfoxide (DMSO). Experiments were performed as described in the [Supporting Information](#).

HCC CELL LINES AND CELL CULTURE

Human HCC cell lines Hep3B, SNU475, SNU761, HepG2, and Huh7 cells were cultured in

Copyright © 2017 by the American Association for the Study of Liver Diseases.

View this article online at wileyonlinelibrary.com.

DOI 10.1002/hep.29237

Potential conflict of interest: The authors who have participated in this study declared that they do not have anything to disclose regarding funding or conflict of interest with respect to this manuscript. But the authors below would like to disclose the following interest. Jung-Hwan Yoon has received a research grant from Bayer HealthCare Pharmaceuticals. Yoon Jun Kim has received research grants from Bristol-Myers Squibb, Roche, JW Creagene, Bukwang Pharmaceuticals, Handok Pharmaceuticals, Hanmi Pharmaceuticals, Yuban Pharmaceuticals, and Pharmaking and has received lecture fees from Bayer HealthCare Pharmaceuticals, Gilead Science, MSD Korea, Yuban Pharmaceuticals, Samil Pharmaceuticals, CJ Pharmaceuticals, Bukwang Pharmaceuticals, and Handok Pharmaceuticals. Su Jong Yu has received a lecture fee from Bayer HealthCare Pharmaceuticals.

ARTICLE INFORMATION:

From the ¹Laboratory for Systems Biology and Bio-inspired Engineering, Department of Bio and Brain Engineering, Korea Advanced Institute of Science and Technology (KAIST), Daejeon, Korea; ²Graduate School of Medical Science and Engineering, KAIST, Daejeon, Korea; ³Department of Pathology, Seoul National University Hospital, Seoul National University College of Medicine, Seoul, Korea; ⁴Department of Internal Medicine and Liver Research Institute, Seoul National University College of Medicine, Seoul, Korea; ⁵Division of Clinical Bioinformatics, Biomedical Research Institute, Seoul National University Hospital, Seoul, Korea; ⁶Department of Surgery, Seoul National University Hospital, Seoul National University College of Medicine, Seoul, Korea.

ADDRESS CORRESPONDENCE AND REPRINT REQUESTS TO:

Kwang-Hyun Cho, Ph.D.
Department of Bio and Brain Engineering, Korea Advanced Institute of Science and Technology (KAIST)

291 Daehak-ro, Yuseong-gu, Daejeon 34141, Republic of Korea
E-mail: ckh@kaist.ac.kr
Tel: +82-42-350-4325

Dulbecco's modified Eagle's medium (WelGENE Inc., Gyeongsan-si, Republic of Korea) with 10% fetal bovine serum and antibiotics (100 units/mL of penicillin, 100 ug/mL of streptomycin, and 0.25 μ g/mL of Fungizone; Life Technologies Corp., Carlsbad, CA) at 37°C in a humidified atmosphere containing 5% CO₂.

REAGENTS

Sorafenib tosylate was purchased from LC Laboratories (Woburn, MA). DMSO, thapsigargin, and propidium iodide (PI) were purchased from Sigma-Aldrich (St Louis, MO). PACMA 31 was purchased from Tocris Bioscience (Bristol, UK). Bortezomib was purchased from Selleck Chemicals (MA).

WESTERN BLOTTING ANALYSIS

Cells were lysed in lysis buffer (20 mM of HEPES [pH 7.2], 150 mM of NaCl, 0.5% Triton X-100, 10% glycerol, 1 μ g/mL of aprotinin, 1 μ g of leupeptin, 1 mM of Na₃VO₄, and 1 mM of NaF). Cell lysates were centrifuged at 13,000 rpm for 15 minutes at 4°C, and the resulting supernatants followed by sodium dodecyl sulfate polyacrylamide gel electrophoresis and immunoblotting analysis. For immunoblotting, anti-phospho-eIF2 α (eukaryotic initiation factor 2 alpha; Cell Signaling Technology, Danvers, MA), anti-PDI (Invitrogen, Carlsbad, CA), and anti- α -actinin (Santa Cruz Biotechnology, Inc., Dallas, TX) were used. The rabbit polyclonal anti-GAPDH (glyceraldehyde 3-phosphate dehydrogenase) antibody was a generous gift from Dr. Ki-Sun Kwon (Korea Research Institute of Bioscience and Biotechnology).

RT-PCR AND qRT-PCR

Total RNA was extracted from cultured cells with RNA-spin (iNtRON, Republic of Korea) and subjected to RT-PCR analysis. RT-PCR was performed using a DiaStar RT kit (Solgent, Republic of Korea) and 2 \times Taq Premix (Solgent) with the following primers for human: C/EBP homology protein (CHOP) forward-1, 5'- TGT CAG CTG GGA GCT GGA AGC -3'; CHOP forward-2, 5'- ACT CTT GAC CCT GCT TCT CTG -3'; CHOP reverse, 5'- ATT CGG TCA ATC AGA GCT CGG -3'; β -actin forward, 5'-AGA GCT ACG AGC TGC CTG AC-3'; β -actin reverse, 5'-AGC ACT GTG TTG GCG TAC AG-3'. GAPDH forward, 5'-CGC TCT CTG CTC CTC CTG TT-3'; GAPDH reverse, 5'-CCA TGG TGT CTG AGC GAT GT-3'. qPCR analysis was performed

using the StepOnePlus (Applied Biosystems, Waltham, MA) with a 20- μ L reaction volume containing complementary DNA (cDNA), primers, and SYBR Master Mix (Applied Biosystems). The data were normalized against GAPDH mRNA in each reaction.

PATHWAY-FOCUSED GENE EXPRESSION PROFILING (PCR-BASED ARRAY)

Pathway-focused gene expression profiling was done using a 96-well human unfolded protein response (UPR) PCR Array, RT² Profiler PCR array (PAHS-089Z, Human UPR RT² Profiler PCR Array; Qiagen, Hilden, Germany). In this array, 84 wells contained all the components required for the PCR reaction in addition to a primer for a single gene in each well. These genes are involved in unfolded protein binding, ER protein folding quality control, regulation of cholesterol metabolism, regulation of translation, ER-associated degradation (ERAD), ubiquitination, transcription factors, protein folding, protein disulfide isomerization, heat shock proteins, and apoptosis. A diluted cDNA template was mixed with the RT² SYBR green master mix (Qiagen), according to the manufacturer's protocol, and loaded onto the 96-well array plate. qPCR analysis was performed using the QuantStudio 5 (Applied Biosystems), by heating the plate to 95°C for 10 minutes, followed by 40 cycles of 95°C for 15 seconds and 60°C for 1 minute. The data were normalized, across all plates, to the following housekeeping genes: hypoxanthine phosphoribosyltransferase 1; beta-2-microglobulin, ribosomal protein, large, P0 (RPLP0); GAPDH; and β -actin.

PLASMID CONSTRUCTION, VIRUS PRODUCTION, AND INFECTION

For lentivirus production, HEK 293T cells were transfected with relevant *lentiviral plasmid* and packaging mix (pLP1, pLP2, and pLP/VSVG) using Lipofectamine (Invitrogen), according to the manufacturer's instructions. For overexpression experiments, the full-length cDNA of PDI was amplified by RT-PCR from total RNA isolated from SNU761 cells using PCR amplification with a forward primer containing *Xba*I site (5'-TCCGTGTCTA-GAATGCT GCGCCGCGCTCTG-3') and a reverse primer containing *Eco*RI site (5'-TGGCTTGAATTCTTAC AGTTCATCTTT-CACAG-3'). The PCR fragment was digested by

XbaI and *EcoRI*, ligated into the pLentiM1.4 lentiviral vector, and confirmed by sequencing. For CHOP knockdown, the plasmid encoding short hairpin RNA (shRNA) targeting CHOP in pLKO.1 was used (Sigma-Aldrich).

NETWORK KERNEL ANALYSIS

To investigate the core structure of a network, the kernel identification algorithm, which condenses a biological network into a smaller one while preserving the input-output dynamics of a network and topological aspects, was adopted as described.⁽⁴⁾ This algorithm recursively replaces the neighborhood subnetwork of each node with a smaller network, which has the same dynamics as the original network, until no further replacement is possible. It is known that essential genes, disease-associated genes, and drug targets are enriched in the reduced kernel network.⁽⁴⁾

THE LOGIC DIAGRAM AND COMPUTATIONAL MODELING OF ER STRESS PATHWAY

An ordinary differential equation (ODE)-based computational model was constructed to investigate the effect of combination treatments. We have applied the step function (θ) to describe the dynamic activities by logical approximation of ODE. Step function is defined as follows.

$$\theta(x > T) = \begin{cases} 1, & x > T \\ 0, & x \leq T \end{cases}$$

where T is the threshold for the node activation.

$$\begin{aligned} \frac{d[MP]}{dt} &= k_1 \text{Sorafenib}(t) - k_2[MP], \\ \frac{d[ER]}{dt} &= k_3[MP] - k_4[ER], \\ \frac{d[PDI, HSP]}{dt} &= k_5(w_1[MP] + w_2[ATF6, IRE1] \\ &\quad - w_3 \text{PDI_inhibitor}(t)) - k_6[PDI, HSP], \\ \frac{d[ATF6, IRE1]}{dt} &= k_7[ER] - k_8[ATF6, IRE1], \\ \frac{d[RMP]}{dt} &= k_9[PDI, HSP] - k_{10}[RMP], \end{aligned}$$

$$\begin{aligned} \frac{d[UPS]}{dt} &= k_{11}(w_4[MP] - w_5[ATF6, IRE1] \\ &\quad - w_6 \text{Proteasome_input}(t) + \\ &\quad w_7[PDI, HSP])\theta(w_4[MP] - w_5[ATF6, IRE1] \\ &\quad - w_6 \text{Proteasome_inhibitor}(t) \\ &\quad > T_1)\theta([PDI, HSP] > T_2) - k_{12}[UPS], \\ \frac{d[CHOP]}{dt} &= k_{13}(w_8[ER] - w_9[RMP] \\ &\quad - w_{10}[UPS]) - k_{14}[CHOP], \\ \frac{d[\text{Apoptosis}]}{dt} &= k_{15}[CHOP] - k_{16}[\text{Apoptosis}] \end{aligned}$$

where [MP], [RMP], and [UPS] denote the misfolded proteins, refolding of misfolded proteins, and ubiquitin-proteasome system, respectively, and $k_1, k_2, k_3, k_4, k_5, k_6, k_7, k_8, k_9, k_{10}, k_{11}, k_{12}, k_{13}, k_{14}, k_{15}$, and k_{16} denote the kinetic parameters, T_1 and T_2 represent the activation threshold of each node, and $w_1, w_2, w_3, w_4, w_5, w_6, w_7, w_8, w_9$, and w_{10} represent the cooperation weights of each node activation, respectively. For the simulation results, we used $k_1 = 0.2, k_2 = 0.2, k_3 = 0.3, k_4 = 0.3, k_5 = 0.3, k_6 = 0.2, k_7 = 0.2, k_8 = 0.2, k_9 = 0.2, k_{10} = 0.2, k_{11} = 0.14, k_{12} = 0.2, k_{13} = 0.2, k_{14} = 0.2, k_{15} = 0.2, k_{16} = 0.2, w_1 = 0.3, w_2 = 0.3, w_3 = 0.3, w_4 = 1.5, w_5 = 1, w_6 = 0.3, w_7 = 0.3, w_8 = 0.8, w_9 = 0.9, w_{10} = 0.5, T_1 = 0$, and $T_2 = 0$.

CELL VIABILITY ASSAYS

HCC cells were seeded into 96-well plate at a density of 6×10^3 cells/well in growth medium, incubated for 24 or 48 hours, and then treated with the indicated concentrations of sorafenib (LC Laboratories) and PACMA 31 (Tocris Bioscience), alone or in combination. Following incubation of the plates for 24 hours, relative cell viability was measured. Briefly, WST-1 solution (Daeillab, Republic of Korea) was added to cells for 30 minutes \sim 2 hours and then measured the absorbance at 450 nm using a xMark Microplate Absorbance Spectrophotometer (Bio-Rad, Hercules, CA).

CELL DEATH ASSAY

To analyze cell death, PI-based assays were performed. IncuCyte ZOOM (Essen Biosciences, Ann Arbor, MI) was used to detect cell death according to the manufacturer's instructions. HCC cells were seeded into a 96-well plate and cultured for 24 hours

(6×10^3 cells/well). Cells were then treated with the indicated concentrations of sorafenib (LC Laboratories) and PACMA 31 (Tocris Bioscience), alone or in combination for 24 hours. After seeding, cells were imaged using IncuCyte ZOOM (Essen Bioscience). To assess cell death, average areas of PI-labeled cells were determined at each time point using the IncuCyte ZOOM analysis software. Images were captured at 3-hour intervals from three separate regions per well with a $20\times$ objective.

ANIMALS AND TREATMENTS

Hep3B cells ($1 \times 10^7/100 \mu\text{L}$) and BD matrigel 100- μL mixture (total, 200 $\mu\text{L}/\text{head}$) were implanted subcutaneously into 5-week-old female Balb/c nude mice. When the average volume of tumors reached 200 mm^3 , mice were randomly divided into four groups ($n = 8$ per group) and then were orally treated with the vehicle (0.5% carboxymethylcellulose sodium, 10 mL/kg) or sorafenib (30 mg/kg) and PACMA 31 (20 mg/kg , intraperitoneal), alone or in combination once-daily for 4 weeks. Tumor volume was calculated as $L \times W^2/2$ (L , length; W , width) every 2-3 days. Mice were maintained on a 12-hour dark/light cycle and fed standard chow. All animal experiments were conducted according to a protocol approved by the Institutional Animal Care and Committee of Seoul National University Hospital.

ELIGIBILITY CRITERIA, TREATMENT REGIMEN, AND ASSESSMENT OF RESPONSE TO SORAFENIB IN PATIENTS WITH HCC

Eligibility criteria for sorafenib therapy were (1) unresectable HCC according to the Barcelona Clinic Liver Cancer (BCLC) staging classification; (2) age <80 years; (3) an Eastern Cooperative Group performance status of 0 or 1; (4) Child-Pugh grade A or B; (5) white blood cell count $>3,000$ cells/ mm^3 , hemoglobin level >10 g/dL , platelet count $>50,000$ cells/ mm^3 ; and (6) serum total bilirubin <3.0 mg/dL , serum transaminases <200 IU/L , and serum creatinine <1.5 mg/dL . These eligibility criteria were based on the vulnerability to adverse side effects. Diagnosis of HCC was confirmed based on hematoxylin-eosin staining of histopathological specimens in all patients. Sorafenib was given orally at a dose of 400 mg twice-daily. Treatment interruptions and up to two dose reductions (first to 400 mg once-daily and then to 400 mg every 2 days) were permitted for drug-related adverse effects (the Common Terminology Criteria for

Adverse Events [version 3]).⁽⁵⁾ Treatment was continued until the radiological progression, as defined by the modified Response Evaluation Criteria in Solid Tumors (mRECIST).⁽⁶⁾ Assessed by contrast-enhanced computed tomography or magnetic resonance imaging every 6-8 weeks, therapeutic response to sorafenib was defined according to the criteria of mRECIST. Complete response (CR) was defined as disappearance of all arterial-enhancing lesions. Partial response (PR) was defined as at least a 30% decrease in the sum of the longest diameter of viable target lesions, taking as reference the baseline sum of the diameters of target lesions. Progressive disease (PD) was defined as at least 20% increase in the sum of the diameters of viable target lesions, taking as reference the smallest sum of the diameters of viable target lesions recorded since treatment started. Stable disease (SD) was defined as any cases that do not meet either PR or PD. When the response achieved for intrahepatic HCC differed from that for extrahepatic HCC, the worse response was determined as the achieved response. Assessment of response was introduced best overall response of mRECIST across all assessment time points.

IMMUNOHISTOCHEMICAL ANALYSIS

Anti-PDI antibody (clone RL90) for immunohistochemistry (IHC) was purchased from Abcam (Cambridge, UK), and immunostaining was done using the Ventana Optiview system (Roche Diagnostics, Mannheim, Germany). Slides were scanned by Aperio ScanScope CS2 (Leica Biosystems, Nussloch, Germany), and image files of each core were obtained. PDI immunopositivity was calculated by the Positive Pixel Count Algorithm of the Aperio ImageScope (Leica Biosystems). Two or more cores per case were examined, and the highest value was used as a representative value.

STATISTICAL ANALYSIS

The Mann-Whitney U test and the Kruskal-Wallis test were used to analyze differences between the different groups. The chi-square test and Fisher's exact test were used for categorical data. To define the best cut-off value for predicting outcome, time-dependent receiver-operating characteristic (ROC) curves for censored survival data were constructed.⁽⁷⁾ The best cut-off value was adopted when it had the maximal sum of sensitivity and specificity. Time to progression (TTP) was calculated from the first day of sorafenib to PD. Overall survival (OS) was calculated from the date of

commencement of sorafenib to the date of death or last contact. Conventional clinical factors at the time of entry into the study and immunopositivity for PDI were analyzed to identify variables that influenced survival as determined by the Kaplan–Meier method and compared by the log-rank test. Step-wise, multivariate analysis was performed using the Cox proportional hazards model to identify independent variables that influenced survival. Factors found to be significantly related to outcome by univariate analysis were included in the multivariate analysis. All statistical analyses were performed using SPSS software (version 19.0; SPSS, Inc., Chicago, IL), and *P* values of <0.05 were considered significant.

Results

SORAFENIB-RESPONSIVE mRNA CHANGES INDICATE THAT APOPTOSIS CAN BE INDUCED BY PROTEOTOXIC STRESS FROM SORAFENIB

To identify the action mechanism and the resistance mechanism of sorafenib, the transcriptomic changes of HCC cell lines (SNU761, Huh7, Hep3B, and HepG2) before and after sorafenib treatment were analyzed. Although their sensitivity to sorafenib was generally similar, SNU761 and Huh7 cells were relatively resistant to sorafenib compared to Hep3B and HepG2 cells (Supporting Fig. S1). To find out biologically relevant gene sets that significantly change, gene list functional enrichment analysis and gene set enrichment analysis were done (Supporting Materials and Methods).

It was shown that the UPR gene set was significantly changed in SNU761, Huh7, and Hep3B, but to a lesser degree in HepG2 (Supporting Files S1 and S2). This result raises the possibility that sorafenib causes proteotoxic stress, which may lead to apoptosis or resistance in some groups of HCC cell lines.

To confirm this hypothesis, western blotting for phospho-eIF2 α , which is a marker of protein kinase RNA-like endoplasmic reticulum kinase (PERK) axis activation, crucial in UPR, was conducted and it was shown that sorafenib induces UPR. In addition, RT-PCR of CHOP (DNA-damage-inducible transcript 3), which is known to be a marker for ER stress-induced apoptosis, suggests that ER stress-induced apoptosis might be brought about by sorafenib (Fig. 1). To confirm that hypothesis, cell viability assays of Hep3B cells expressing scrambled shRNA or CHOP

shRNA were performed. Sorafenib-induced apoptosis was reduced in CHOP knockdown cells compared to control cells (Supporting Fig. S2).

THE EFFECT OF SORAFENIB ON ER STRESS NETWORK

To clarify the effect of sorafenib on ER stress pathway and identify molecules that can mitigate the efficacy of sorafenib and cause resistance to apoptosis, we constructed a signaling network model of ER stress (Supporting Fig. S3). This network model is composed of three parts. One is the UPR part that is composed of UPR signal transducers being activated by the accumulation of unfolded or misfolded protein. The others are the protein refolding part and the ERAD part that relieve the proteotoxic stress by refolding or degrading misfolded proteins, which results in cell survival.

To explore this network, a qRT-PCR-based array for 84 key molecules constituting this pathway was performed in SNU761 cell lines (Fig. 2; Supporting Table S1). Thirty-seven of 84 molecules were significantly up-regulated when sorafenib was treated, whereas none was down-regulated (Supporting Table S1). When these changes were displayed on the network model, both the UPR and ERAD parts were found to be activated (Supporting Fig. S3). Molecules for ER protein folding (Fig. 2C) and ubiquitin-proteasome pathway (Fig. 2D,E) were up-regulated, which results in resistance to apoptotic effects of sorafenib. To test whether this phenomenon occurs in another cell line, the same experiment was performed in HepG2 and Huh7 cell lines. The HepG2 cell line was chosen because it showed a weaker UPR than other cell lines from microarray experiments, whereas the Huh7 cell line showed similar responses with the SNU761 cell line. UPRs were not apparent in the HepG2 cell line (Supporting Fig. S4). But the Huh7 cell line showed similar reactions with the SNU761 cell line in qRT-PCR analysis (Supporting Fig. S5). These results suggest that ER stress is induced depending on cellular contexts.

DISCOVERY OF A TARGET MOLECULE FOR INCREASING THE EFFICACY OF SORAFENIB

To identify candidates for the combination therapy with sorafenib, two different approaches were used. First, we applied the kernel identification algorithm, which elucidates essential nodes for network dynamics. The input set is the ER stress pathway network that consists of 20 nodes and 34 links (Supporting Fig. S6A). By the

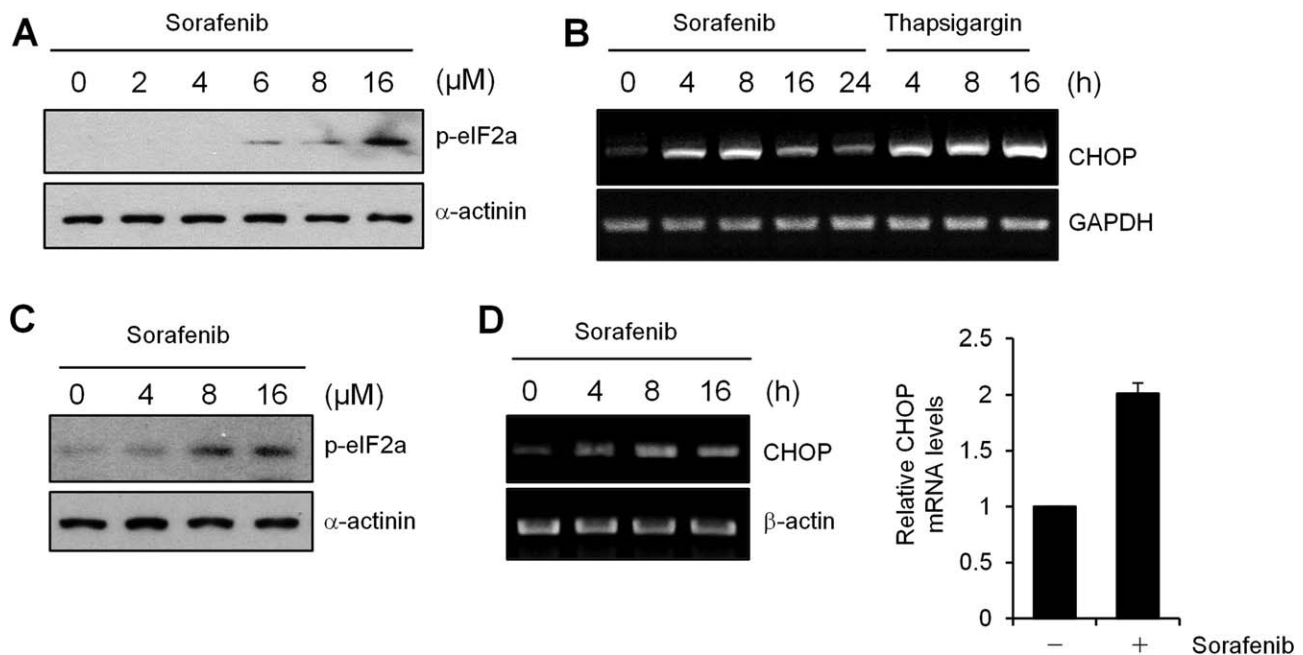


FIG. 1. Sorafenib induces ER stress in HCC cells. (A) Immunoblotting of phospho-eIF2a (p-eIF2a) from SNU761 cells that were treated with the indicated concentration of sorafenib for 24 hours. (B) CHOP mRNA expression in SNU761 cells was analyzed by RT-PCR. Thapsigargin, an ER stress inducer, was used as a positive control and GAPDH was used as a loading control. (C) Immunoblotting of phospho-eIF2a from Huh7 cells that were treated with the indicated concentration of sorafenib for 24 hours. (D) Left, CHOP mRNA expression in Huh7 cells were analyzed by RT-PCR. β -actin was used as a loading control; right, CHOP mRNA expression was quantified by real-time PCR.

kernel identification algorithm, it was condensed into the smaller network with six nodes and 10 links (Supporting Fig. S6B). In this condensed network, heat shock proteins (HSPs) and PDI are found to be the crucial nodes against apoptosis. Because HSPs are the family of several molecules that cannot be completely blocked by one inhibitor, whereas PDI inhibitor can hinder the enzymatic activities of the broad ranges of the PDI family, PDI was given the first priority as a target molecule.

Second, because inhibition of proteasome by an inhibitor, such as bortezomib, has been known to cause proteotoxic stress and show synergistic effects with sorafenib,⁽⁸⁾ the comparison between the effect of proteasome inhibitor and that of PDI inhibitor was conducted *in silico* and *in vitro*. An ordinary differential equation model based on the logical approximation was constructed and the effect of each inhibitor was simulated (Fig. 3). PDI inhibition showed much more synergy than proteasome inhibition (Fig. 3B), and similar results were obtained with diverse coefficient values (Supporting Fig. S7).

To confirm those *in silico* results, cell viability assay and apoptosis assay were performed in multiple cell lines (Fig. 4). Whereas bortezomib demonstrated the

mild additive effect with sorafenib (Supporting Fig. S8), PACMA 31 revealed the synergistic effects.

THE EFFECT OF COMBINED TREATMENT WITH PACMA 31 ON ER STRESS NETWORK

A qRT-PCR-based array for 84 key molecules constituting ER stress network was performed (Fig. 5). Whereas molecules intensifying apoptosis were up-regulated in the combination group (Fig. 5A,B), antiapoptotic molecules, such as X-box binding protein (XBP1) and mesencephalic astrocyte-derived neurotrophic factor (MANF), were down-regulated, even in comparison to the control group. Molecules participating in protein folding and ERAD were down-regulated in the combination treatment group compared to the sorafenib group (Fig. 5C-F), except those that are involved in the activation of PDI (ER degradation-enhancing alpha-mannosidase-like 1 [EDEM1] and endoplasmic oxidoreductin-1-like protein [ERO1L]), whereas there were no such effects in the PACMA 31 single-treatment group. When these changes were displayed on the

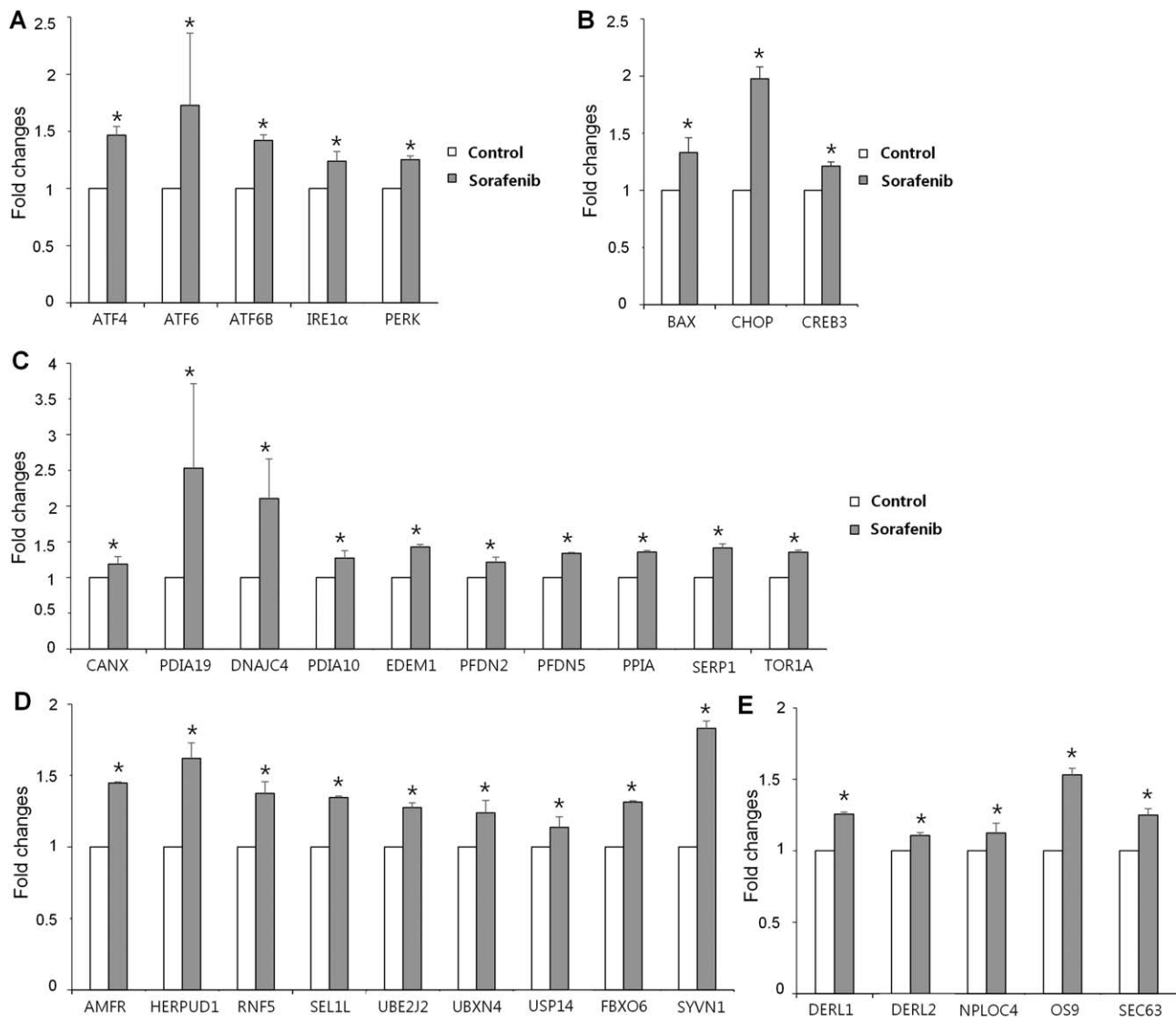


FIG. 2. Effect of sorafenib on the gene expression change of molecules in ER stress network. qRT-PCR experiments on SNU761 cells were done twice in 2 μ M of sorafenib and two or four times in 4 μ M of sorafenib. *P* values were obtained through paired *t* test or Wilcoxon signed-ranks test and descriptive statistics was calculated from 4- μ M tests. (A) UPR signal transducers. (B) Molecules involved in apoptosis. (C) Molecules participating in ER protein folding and quality control. (D) Ubiquitin-proteasome system. (E) Molecules involved in retrotranslocation ($*P < 0.05$). Abbreviations: AMFR, autocrine motility factor receptor; ATF, activating transcription factor 4; BAX, BCL2-associated X, apoptosis regulator; CANX, calnexin; CREB3, cAMP-responsive element-binding protein 3; DERL, derlin; DNAJC4, DnaJ heat shock protein family (Hsp40) member C4; EDEM1, ER degradation enhancing alpha-mannosidase like protein 1; FBXO6, F-box only protein 6; HERPUD1, homocysteine inducible ER protein with ubiquitin like domain 1; IRE1 α , inositol-requiring enzyme 1 alpha; NPLOC4, NPL4 homolog, ubiquitin recognition factor; OS9, osteosarcoma amplified 9, endoplasmic reticulum lectin; PDIA, protein disulfide isomerase family A; PFDN, prefoldin; PPIA, peptidylprolyl isomerase A; RNF5, ring finger protein 5; SEC63, SEC63 Homolog, protein translocation regulator; SEL1L, SEL1L ERAD E3 Ligase Adaptor Subunit; SERP1, stress associated endoplasmic reticulum protein 1; SYVN1, synoviolin 1; TOR1A, torsin family 1 member A; UBE2J2, ubiquitin conjugating enzyme E2 J2; UBXN4, UBX domain protein 4; USP14, ubiquitin specific peptidase 14.

network model, we found that the ERAD part (right) and protein refolding (center) were turned off whereas the apoptotic pathway was activated in the UPR part (Supporting Fig. S9).

In the case of HepG2, UPR was not evident upon sorafenib treatment (Supporting Fig. S4), but synergistic cytotoxicity was observed with PACMA 31 like other cell lines (Fig. 4). It was shown that c-Jun N-

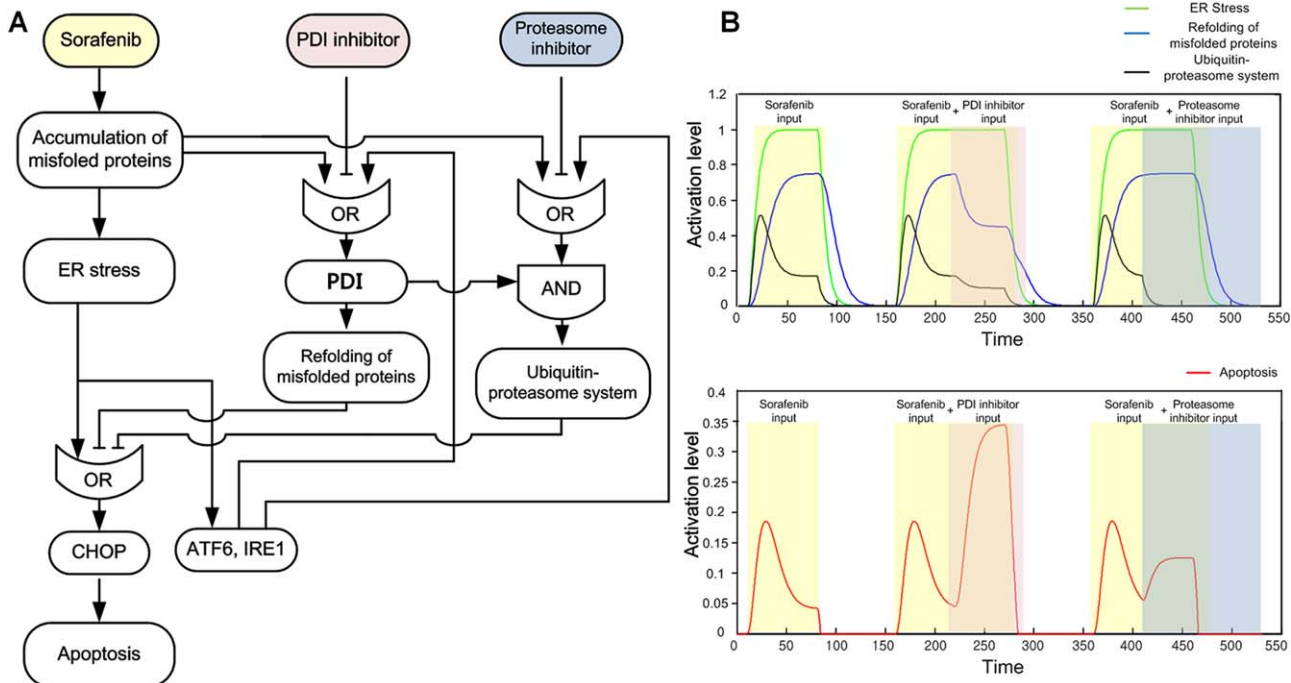


FIG. 3. Logic diagram of ER stress network and the simulation of PDI or proteasome inhibition. (A) Logic diagram of ER stress network and its inhibitors. (B) Simulation results of the model based on logical approximation of ODEs (see Materials and Method for details). Abbreviations: ATF6, activating transcription factor; a.u., arbitrary unit; IRE1, inositol-requiring enzyme 1.

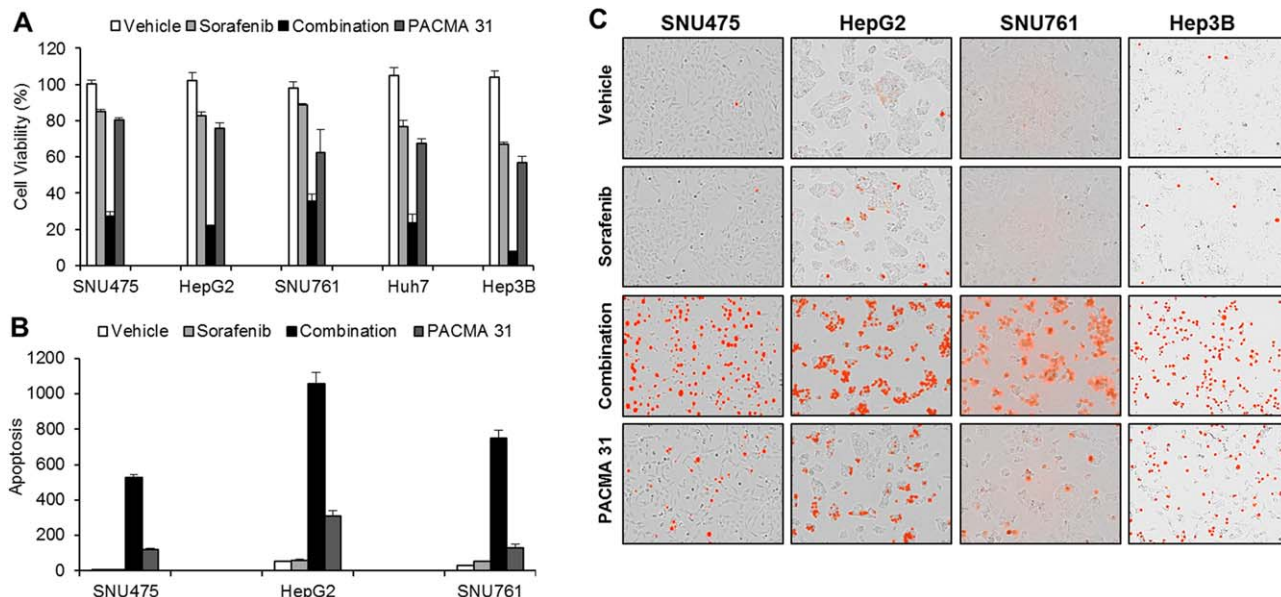


FIG. 4. PACMA 31 enhances sorafenib-induced cytotoxicity. HCC cells were treated with 4 μ M of sorafenib alone, 0.4 μ M of PACMA 31 alone, or in combination for 24 hours. (A) Cell viability assay in Hep3B, SNU475, HepG2, SNU761, and Huh7 cells. Experiments were repeated in triplicates. (B) Apoptosis assay in SNU475, HepG2, and SNU761 cells. Results are presented by means \pm SEM (error bars). (C) To analyze cell death, PI was added to cells at a final concentration of 1 μ g/mL. Images were taken 6 hours after each treatment.

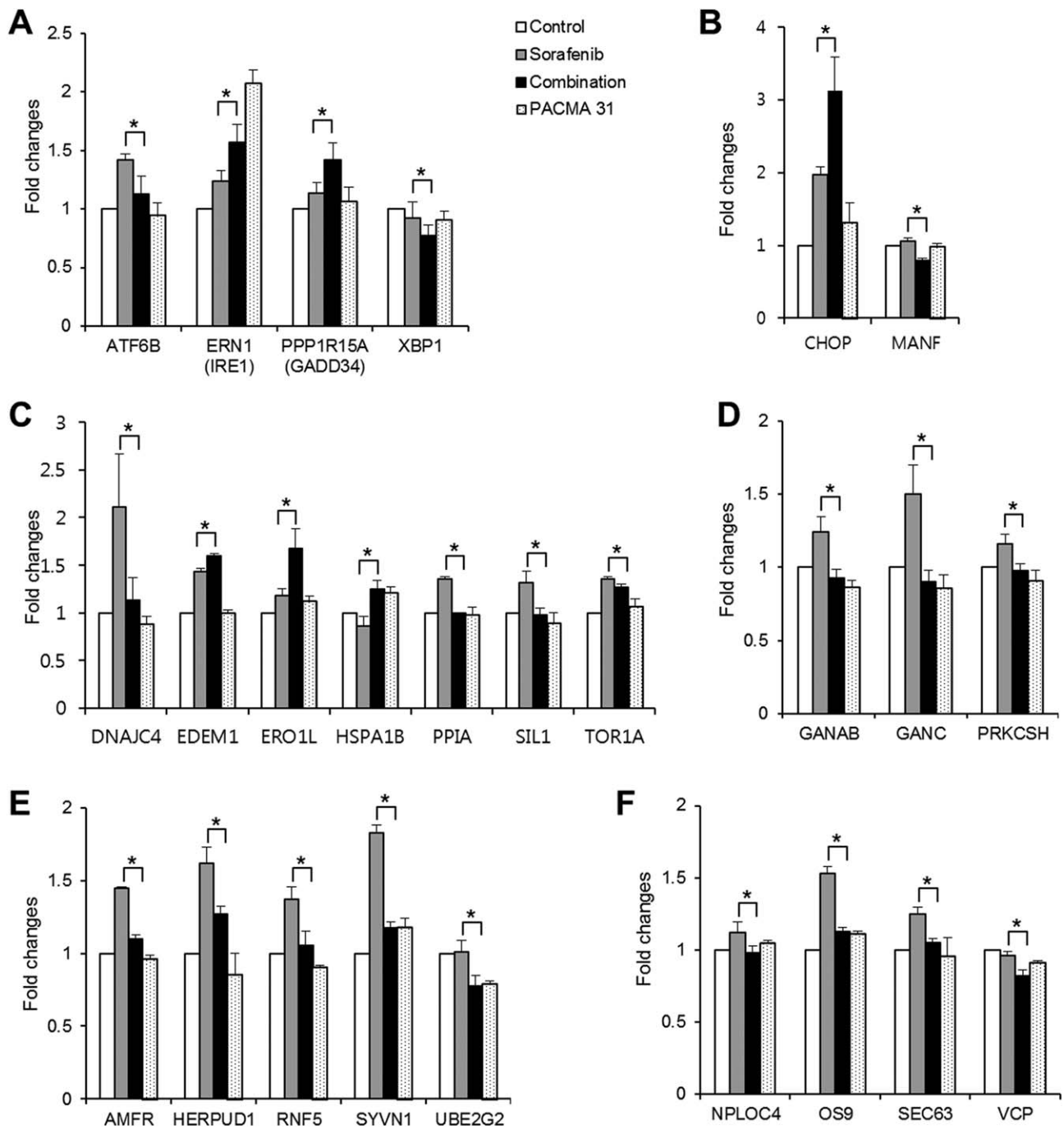


FIG. 5. Comparison between sorafenib alone, combination treatment, and PACMA 31 alone on gene expression change of molecules in the ER stress network of SNU761 cells. (A) UPR signal transducers. (B) Molecules involved in apoptosis. (C) Molecules participating in ER protein folding and quality control. (D) Glycoprotein processing. (E) Ubiquitin-proteasome system. (F) Molecules involved in retrotranslocation (**P* < 0.05). Abbreviations: AMFR, autocrine motility factor receptor; ATF6B, activating transcription factor 6B; DNAJC4, DnaJ heat shock protein family (Hsp40) member C4; EDEM1, ER degradation enhancing alpha-mannosidase like protein 1; ERN1, endoplasmic reticulum to nucleus signaling 1; GANAB, glucosidase II alpha subunit; GANC, glucosidase alpha, neutral C; HERPUD1, homocysteine inducible ER protein with ubiquitin like domain 1; HSPA1B, heat shock protein family A (Hsp70) member 1B; IRE1, inositol-requiring enzyme 1; NPLOC4, NPL4 homolog, ubiquitin recognition factor; OS9, osteosarcoma amplified 9, endoplasmic reticulum lectin; PPIA, peptidylprolyl isomerase A; PPKCSH, glucosidase-II; PPP1R15A, protein phosphatase 1 regulatory subunit 15A; RNF5, ring finger protein 5; SEC63, SEC63 Homolog, protein translocation regulator; SIL1, SIL1 nucleotide exchange factor; SYVN1, synoviolin 1; TOR1A, torsin family 1 member A; UBE2G2, ubiquitin conjugating enzyme E2 G2; VCP, valosin-containing protein.

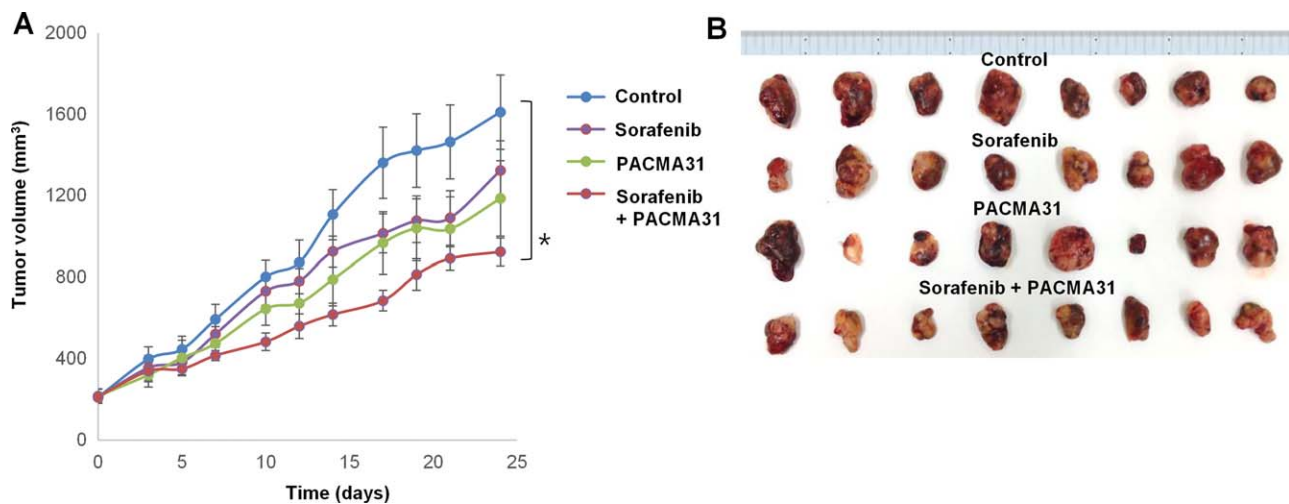


FIG. 6. Combination treatment with PACMA 31 suppressed growth of Hep3B xenografts *in vivo*. Female nude mice with Hep3B cells were divided into four groups and treated as described. (A) Change of tumor volume. (B) Pictures of tumors resected from mice.

terminal kinase (JNK) and CHOP are induced by the combinatorial treatment of sorafenib and PACMA 31 (Supporting Fig. S10).

THE EFFICACY OF THE COMBINED TREATMENT WITH PACMA 31 *IN VIVO*

We further evaluated the effect of the combined treatment with PDI inhibitor using a xenograft mice model. The combined treatment significantly reduced tumor volume, whereas the others did not in comparison with the control group (Fig. 6; two-way repeated-measure analysis of variance, $P < 0.05$).

HIGH PDI EXPRESSION CAN PREDICT A POOR CLINICAL OUTCOME AFTER SORAFENIB TREATMENT IN PATIENTS WITH HCC

To find out the relationship between PDI expression and clinical outcome in HCC patients receiving sorafenib, we analyzed PDI immunopositivity in HCC patients who have been treated with sorafenib. IHC analysis for PDI protein expression in our HCC patient cohort ($n = 95$) demonstrated that PDI expression was increased in tumor tissue of 59 cases (62.1%), whereas 36 (37.9%) showed the decrease of PDI expression

compared to adjacent nontumor tissue (Supporting Table S2). Among them, CR and PR were achieved in 2 of 95 (2.1%) and 1 of 95 (1.1%) of cases, respectively. SD was noted in 8 of 95 patients (8.4%) and disease control (CR+PR+SD) was achieved in 11 of 95 (11.6%). PD was noted in 84 of 95 (88.4%) cases. The low-PDI-expression group showed a significantly better response (disease control) to sorafenib compared to the high-PDI-expression group (22.2% vs. 5.1%, respectively; $P = 0.018$; Table 1). These results suggest that PDI might be involved in the response to sorafenib.

We then performed survival analysis. Median TTP was 2.2 months (range, 0.1-38.7). Cumulative progression-free survival rates at 3, 6, and 12 months were 40.8%, 19.7%, and 6.6%, respectively. Forty-seven patients were alive at the end of the observation period, whereas 47 had died. Median survival time was 10.0 months (range, 1.0-76.0). Cumulative survival rate at 3, 6, and 12 months was 85.4%, 63.5%, and 37.9%, respectively.

The impact of PDI expression in HCC tissues on the prognosis of patients treated with sorafenib was examined. The Kaplan–Meier method demonstrated significant prolongation of TTP in the low-PDI-expression group, compared to the high-PDI-expression group (Fig. 7A; $P = 0.035$). The prognostic factors for TTP in multivariate analysis were high PDI expression (hazard ratio [HR], 1.833; 95% confidence interval [CI], 1.143-2.937; $P = 0.012$), age (HR, 0.558; 95% CI, 0.339-0.918; $P = 0.022$),

TABLE 1. Response of HCC Patients to Sorafenib According to the PDI Expression Level

		PDI Expression Level		No.
		Low (Grade 0-1)	High (Grade 2-3)	
Clinical response	CR+PR+SD	8	3	11
	No response	28	56	84
	Response rate, %	22.2	5.1	95
<i>P</i> value		0.018 (Fisher's exact test)		

lymph node involvement (HR, 2.368; 95% CI, 1.335-4.200; *P* = 0.003), and presence of metastasis (HR, 3.478; 95% CI, 1.559-7.761; *P* = 0.002; [Supporting Table S3](#)). A significant prolongation of OS in the low-PDI-expression group compared to the high-PDI-expression group (*P* = 0.024; Fig. 7B) was also found. The prognostic factors for OS in multivariate analysis were high PDI expression (HR, 1.878; 95% CI, 1.107-3.184; *P* = 0.019), poor Child-Pugh score (HR, 1.966; 95% CI, 1.349-2.864; *P* < 0.001), high number of tumors (HR, 1.109; 95% CI, 1.037-1.186; *P* = 0.003), and lymph node involvement (HR, 2.135; 95% CI, 1.148-3.971; *P* = 0.017; [Supporting Table S4](#)).

Discussion

In this study, the gene expression changes upon sorafenib treatment were analyzed and it was found that proteotoxic stress and UPR are mainly associated with

the resistance mechanism of sorafenib. Moreover, *in vitro* study showed that sorafenib brings about ER stress-induced apoptosis, but its effect was attenuated by activation of protein refolding and ERAD pathway. Network analysis and *in silico* simulation to discover a target molecule that can block those compensatory responses revealed that PDI can be a candidate. Furthermore, *in vitro* and *in vivo* experiments proved that PDI inhibition shows the synergistic effect with sorafenib. We also found that PDI expression in HCC patients predicts resistance to sorafenib treatment.

PDI is one of the most abundant soluble proteins in the ER and acts as a reductase, an oxidase, and an isomerase as well as a molecular chaperone.⁽⁹⁾ UPR is an important mechanism to sustain homeostasis between cell survival and apoptosis resulting from misfolded proteins.^(10,11) Given that PDI exerts key functions in protein folding, refolding, and even retrotranslocation for ERAD,⁽¹²⁾ blocking this activity can be a way to hinder the mitigation of ER stress, which

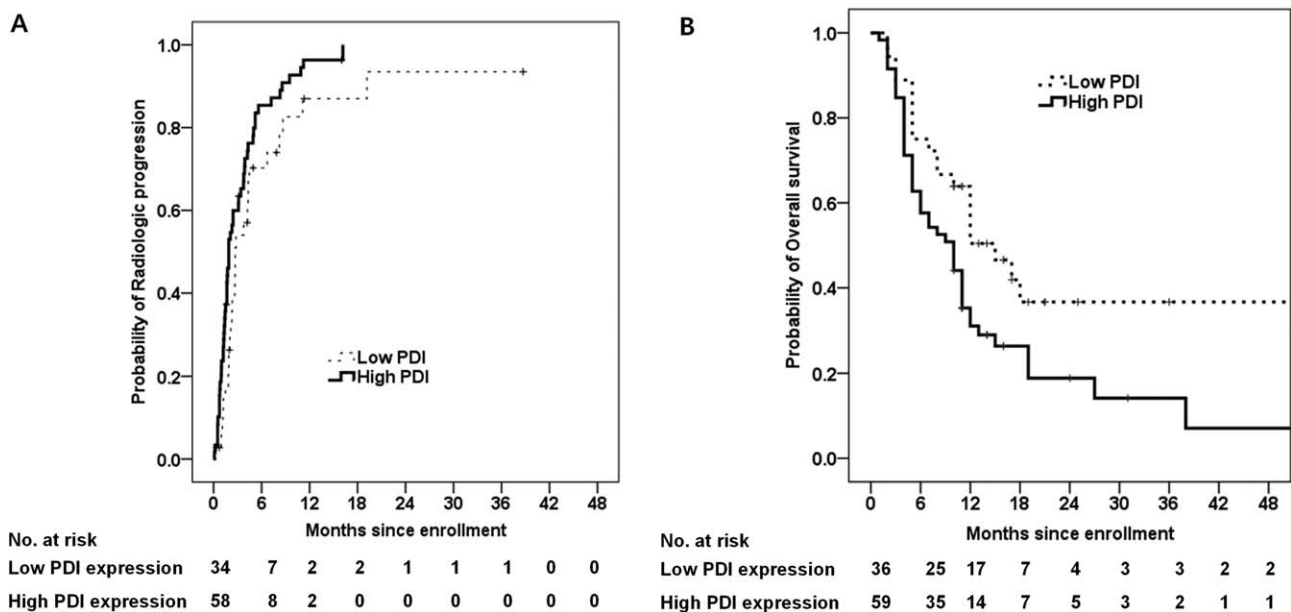


FIG. 7. Survival analysis according to the PDI expression level. (A) Time to progression. (B) Overall survival.

leads to cell death.⁽¹³⁾ Recent studies showed that PDI plays a crucial role in cancer survival and progression.⁽¹⁴⁻¹⁶⁾ In addition, it was reported that PDI mediates resistance to cytotoxic chemotherapy.⁽¹⁷⁾ In our previous work, expression of PDI was increased in HCC compared to nontumor tissue and high PDI expression level in HCC tissue adversely affected clinical outcomes in HCC patients.⁽¹⁸⁾ The results of this study suggest that PDI exerts an important role in resistance to sorafenib. But when we performed PDI overexpression experiments in *in vitro*, it seemed that PDI overexpression had little correlation with response to sorafenib, but appeared to make HCC cells more sensitive to the combination treatment of sorafenib and PDI inhibitor (Supporting Fig. S11). In addition to the low dosage of sorafenib in our study, some overexpression may not significantly affect the overall activity of PDI in *in vitro*, depending on cellular context, given that PDI is an enzyme. In some cell lines, it has been shown that overexpression of PDI abrogated the effect of chemotherapeutic agents.^(17,19) Maybe its effect will be diverse depending on drug dosage, cell types, and cellular context. However, *in vivo*, sorafenib has been known to induce tumor hypoxia through an antiangiogenic effect,⁽²⁰⁾ which leads to more exposure to ER stress that is difficult to cope with.⁽²¹⁾ In this case, PDI overexpression can be helpful for cancer cells to survive. Indeed, in our patient cohort, high PDI expression in HCC tissues is significantly correlated with sorafenib resistance and predicts poor clinical outcomes after sorafenib treatment.

Cancer cells have developed several ways to compensate for stressful conditions.⁽²²⁾ If we exploit those attributes, it will be possible to increase the vulnerability of cancer to anticancer drugs.⁽¹⁹⁾ In this study, we found that PDI can be a useful target.

In the course of searching a proper target molecule, we used two approaches: network kernel analysis and *in silico* simulations. First, network kernel analysis reduces the complex network to a simpler network while maintaining the original dynamics.⁽⁴⁾ Given that it has been known that the remaining genes in such a reduced network are enriched with drug targets and the synthetic lethal pairs, the reduced kernel network can be useful in searching for a potential target. Second, because it has been known that *in silico* simulations based on ODE modeling can be useful in the quantitative analysis of the effect of targeted inhibitor,⁽²³⁾ we predicted that PDI inhibition can be more effective than proteasome inhibition from the simulation analysis. This might be because PDI is a hub node

connecting the UPR part, protein refolding part, and ERAD part. It should be noted that PDI plays multiple roles, including the thiol-disulfide oxidoreductase, disulfide isomerase, and molecular chaperone.⁽²⁴⁾

In the qRT-PCR experiment for ER stress network, some questions can be raised. Sorafenib increases overall expression of molecules belonging to the UPR signal transducer, chaperones, and ERAD system in SNU761 and Huh7 cells. But when combined with PDI inhibitor, a majority of chaperones and ERAD proteins are down-regulated together with antiapoptotic molecules including XBP1 and MANF. The reason why such transcriptional effects occur remains as a challenging issue. In our opinion, those expression changes might have been originated from CHOP induction by the combinatorial effect of sorafenib and PDI inhibition through uncompensated ER stress. Unfolded or misfolded client proteins can impose such ER stress, which leads to cell death in pathological conditions. The transcription factor, CHOP, is activated by ER stress, and CHOP directly activates growth arrest and DNA damage-inducible protein 34 (GADD34), which promotes ER client protein biosynthesis, but not ERAD or UPR proteins.⁽²⁵⁾ Given that endogenous reference genes of qRT-PCR analysis could be also included in the ER client proteins and might be induced by CHOP, it appears that UPR proteins, including ERAD molecules, seem to be relatively less expressed. It should be unveiled, in future studies, whether this phenomenon is caused by indirect effect through the uncompensated ER stress or the combination treatment directly regulates these molecules by other pathways. In the case of HepG2 cells, sorafenib alone seems to cause cell death in other ways without going through ER stress. However, when combined with PDI inhibitor, expression of JNK and CHOP is highly increased (Supporting Fig. S10). Given that JNK is also a well-known inducer of ER stress-induced apoptosis,⁽²⁶⁾ it seems that the combination treatment enhances apoptosis in HepG2 cells through the JNK-BCL2 (B-cell lymphoma 2) axis, unlike other cell lines. Further detailed mechanisms should be clarified in future studies.

In our patient cohort, PDI expression predicts resistance to sorafenib and is significantly correlated with OS and TTP after sorafenib treatment. To verify this result, additional studies are needed using other patient cohorts and the relationship with other known resistance factors, such as hypoxia-inducible factor 1 alpha and VEGFR, should be investigated.^(27,28) And, testing a patient-derived xenograft model may be a

valuable method to confirm the efficacy of the combination treatment with PDI inhibitor.

In conclusion, PDI is an effective target for overcoming resistance to sorafenib treatment and can also be a predictive marker to predict sorafenib responsiveness and clinical outcomes.

Acknowledgments: The pLentiM1.4 lentiviral vector was kindly provided by Dr. Y.-S. Kim (Chungnam National University, Daejeon, Korea). The authors thank Bo Hyun Kim for sharing her knowledge and ideas. The authors thank Young Youn Cho, Sung-Hee Lee, Soo-Mi Lee, and Hyo Ju Jang for their technical support and assistance in preparing the manuscript.

REFERENCES

- 1) Kostner AH, Sorensen M, Olesen RK, Gronbaek H, Lassen U, Ladekarl M. Sorafenib in advanced hepatocellular carcinoma: a nationwide retrospective study of efficacy and tolerability. *ScientificWorldJournal* 2013;2013:931972.
- 2) Llovet JM, Ricci S, Mazzaferro V, Hilgard P, Gane E, Blanc JF, et al. Sorafenib in advanced hepatocellular carcinoma. *N Engl J Med* 2008;359:378-390.
- 3) Cervello M, McCubrey JA, Cusimano A, Lampiasi N, Azzolina A, Montalto G. Targeted therapy for hepatocellular carcinoma: novel agents on the horizon. *Oncotarget* 2012;3:236-260.
- 4) Kim JR, Kim J, Kwon YK, Lee HY, Heslop-Harrison P, Cho KH. Reduction of complex signaling networks to a representative kernel. *Sci Signal* 2011;4:ra35.
- 5) Division of Cancer Treatment & Diagnosis, National Cancer Institute, National Institutes of Health, U.S. Department of Health and Human Services. Cancer Therapy Evaluation Program, Common Terminology Criteria for Adverse Events (CTCAE). In. Version 4.0 ed; 2009.
- 6) Lencioni R, Llovet JM. Modified RECIST (mRECIST) assessment for hepatocellular carcinoma. *Semin Liver Dis* 2010;30:52-60.
- 7) Heagerty PJ, Lumley T, Pepe MS. Time-dependent ROC curves for censored survival data and a diagnostic marker. *Biometrics* 2000;56:337-344.
- 8) Chen KF, Yu HC, Liu TH, Lee SS, Chen PJ, Cheng AL. Synergistic interactions between sorafenib and bortezomib in hepatocellular carcinoma involve PP2A-dependent Akt inactivation. *J Hepatol* 2010;52:88-95.
- 9) Xu S, Sankar S, Neamati N. Protein disulfide isomerase: a promising target for cancer therapy. *Drug Discov Today* 2014;19:222-240.
- 10) Walter P, Ron D. The unfolded protein response: from stress pathway to homeostatic regulation. *Science* 2011;334:1081-1086.
- 11) Hetz C. The unfolded protein response: controlling cell fate decisions under ER stress and beyond. *Nat Rev Mol Cell Biol* 2012;13:89-102.
- 12) Vembar SS, Brodsky JL. One step at a time: endoplasmic reticulum-associated degradation. *Nat Rev Mol Cell Biol* 2008;9:944-957.
- 13) Puig A, Lyles MM, Noiva R, Gilbert HF. The role of the thiol/disulfide centers and peptide binding site in the chaperone and anti-chaperone activities of protein disulfide isomerase. *J Biol Chem* 1994;269:19128-19135.
- 14) **Higa A, Mulot A, Delom F, Bouche-careilh M, Nguyen DT, Boismenu D, et al.** Role of pro-oncogenic protein disulfide isomerase (PDI) family member anterior gradient 2 (AGR2) in the control of endoplasmic reticulum homeostasis. *J Biol Chem* 2011;286:44855-44868.
- 15) Tager M, Kroning H, Thiel U, Ansorge S. Membrane-bound protein disulfide isomerase (PDI) is involved in regulation of surface expression of thiols and drug sensitivity of B-CLL cells. *Exp Hematol* 1997;25:601-607.
- 16) Goplen D, Wang J, Enger PO, Tysnes BB, Terzis AJ, Laerum OD, Bjerkvig R. Protein disulfide isomerase expression is related to the invasive properties of malignant glioma. *Cancer Res* 2006;66:9895-9902.
- 17) Tufo G, Jones AW, Wang Z, Hamelin J, Tajeddine N, Esposti DD, et al. The protein disulfide isomerases PDIA4 and PDIA6 mediate resistance to cisplatin-induced cell death in lung adenocarcinoma. *Cell Death Differ* 2014;21:685-695.
- 18) **Yu SJ, Won JK, Ryu HS, Choi WM, Cho H, Cho EJ, et al.** A novel prognostic factor for hepatocellular carcinoma: protein disulfide isomerase. *Korean J Intern Med* 2014;29:580-587.
- 19) **Lovat PE, Corazzari M, Armstrong JL, Martin S, Pagliarini V, Hill D, et al.** Increasing melanoma cell death using inhibitors of protein disulfide isomerases to abrogate survival responses to endoplasmic reticulum stress. *Cancer Res* 2008;68:5363-5369.
- 20) Chang YS, Adnane J, Trail PA, Levy J, Henderson A, Xue D, et al. Sorafenib (BAY 43-9006) inhibits tumor growth and vascularization and induces tumor apoptosis and hypoxia in RCC xenograft models. *Cancer Chemother Pharmacol* 2007;59:561-574.
- 21) Xu C, Bailly-Maitre B, Reed JC. Endoplasmic reticulum stress: cell life and death decisions. *J Clin Invest* 2005;115:2656-2664.
- 22) Hanahan D, Weinberg RA. Hallmarks of cancer: the next generation. *Cell* 2011;144:646-674.
- 23) **Won JK, Yang HW, Shin SY, Lee JH, Heo WD, Cho KH.** The crossregulation between ERK and PI3K signaling pathways determines the tumoricidal efficacy of MEK inhibitor. *J Mol Cell Biol* 2012;4:153-163.
- 24) Ali Khan H, Mutus B. Protein disulfide isomerase a multifunctional protein with multiple physiological roles. *Front Chem* 2014;2:70.
- 25) Marciniak SJ, Yun CY, Oyadomari S, Novoa I, Zhang Y, Jungreis R, et al. CHOP induces death by promoting protein synthesis and oxidation in the stressed endoplasmic reticulum. *Genes Dev* 2004;18:3066-3077.
- 26) **Szegezdi E, Logue SE, Gorman AM, Samali A.** Mediators of endoplasmic reticulum stress-induced apoptosis. *EMBO Rep* 2006;7:880-885.
- 27) **Liang Y, Zheng T, Song R, Wang J, Yin D, Wang L, et al.** Hypoxia-mediated sorafenib resistance can be overcome by EF24 through Von Hippel-Lindau tumor suppressor-dependent HIF-1alpha inhibition in hepatocellular carcinoma. *HEPATOLOGY* 2013;57:1847-1857.
- 28) **Peng S, Wang Y, Peng H, Chen D, Shen S, Peng B, et al.** Autocrine vascular endothelial growth factor signaling promotes cell proliferation and modulates sorafenib treatment efficacy in hepatocellular carcinoma. *HEPATOLOGY* 2014;60:1264-1277.

Author names in bold designate shared co-first authorship

Supporting Information

Additional Supporting Information may be found at onlinelibrary.wiley.com/doi/10.1002/hep.29237/supinfo.